Research Square

Preprints are preliminary reports that have not undergone peer review.
They should not be considered conclusive, used to inform clinical practice,
or referenced by the media as validated information.

Recurrent flooding beyond the reach of flood risk management in New York City

CE BIAN

cecbian@outlook.com

Lamont--Doherty Earth Observatory, Columbia University, Palisades, NY, USA https://orcid.org/0009-0003-7721-5552

David Bresch

Institute for Environmental Decisions, ETH Zurich, Zurich, Switzerland

Tian Zheng

Department of Statistics, Columbia University, New York, NY, USA

Article

Keywords:

Posted Date: November 25th, 2026

DOI: https://doi.org/10.21203/rs.3.rs-11696177/v1

License: This work is licensed under a Creative Commons Attribution 4.0 International License.
Read Full License

Additional Declarations: There is **NO** Competing Interest.

Recurrent flooding beyond the reach of flood risk management in New York City

Ce Bian[1,2,*], David N. Bresch[3,4], Tian Zheng[5]

[1]Lamont–Doherty Earth Observatory, Columbia University, Palisades, NY, USA
[2]Columbia Climate School, Columbia University, New York, NY, USA
[3]Institute for Environmental Decisions, ETH Zurich, Zurich, Switzerland
[4]Federal Office of Meteorology and Climatology MeteoSwiss, Zurich-Airport, Switzerland
[5]Department of Statistics, Columbia University, New York, NY, USA
[*]Corresponding author: cebian@ldeo.columbia.edu

Abstract

Urban flood risk in the United States is managed through flood maps, drainage standards and public insurance, but these instruments need not represent where and how often flooding occurs. We integrate observations, simulations, exposure data and insurance records to examine this alignment in New York City. Losses from rare storm surges concentrate along the waterfront, where tidal flooding also recurs, while rainfall flooding extends inland. Tidal sensors record flooding on a median of four days a year, and 93% of the extreme-rainfall footprint lies outside the federal flood zone, exposing basement homes and subway stations. Even within the mapped zone, frequent tidal flooding remains insufficiently addressed, while insurance covers a declining share of losses as event losses grow. These findings reveal a gap between recurrent flood exposure and existing risk management. A place-based measure of flood frequency, observable from street sensors, could help close this gap.

Urban flood risk extends beyond rare coastal storm surges. In September 2021, the remnants of Hurricane Ida dropped more than three inches of rain on New York City in an hour and killed 14 people, 11 of them by drowning in basement apartments[1]. The homes were reported to lie in areas that the federal flood map marks as having minimal flood hazard[2]. Street-level observations now reveal flooding that conventional assessments can overlook: since 2020, a network that has grown to 479 sensors[3] has recorded tidal flooding that recurs several times a year at some shoreline sites, and occasional rainfall flooding farther inland. Such flooding threatens below-grade homes, including informal basement apartments housing low-income renters[4,5], and underground subway stations. Building-loss estimates alone cannot describe the full consequences for their occupants and users. Rainfall flooding is largely absent from federal flood maps[6] and rarely managed comprehensively in cities[7], while chronic tidal flooding is becoming more frequent[8,9], with cumulative costs that can rival those of rare events[10]. These observations raise

a question: do the instruments that guide flood decisions represent the flooding that residents repeatedly experience?

Flood decisions draw on hazard maps, estimates of loss and engineering design standards. Coastal and riverine flood maps delineate inundation associated with specified probabilities, most prominently the 1-in-100-year flood, while expected annual loss integrates losses across event probabilities and informs insurance pricing and cost–benefit assessments of flood defences[11–14]. In New York City, substantial work after Hurricane Sandy revised surge water-level frequencies[15–18], developed surge loss models[12,19] and produced preliminary revisions of the federal flood map[20]. Three instruments translate flood information into decisions. The Federal Emergency Management Agency (FEMA) delineates the Special Flood Hazard Area (hereafter the flood zone), which is used to establish insurance requirements and floodplain development standards[20]. Drainage design standards specify the rainfall intensity that sewers are designed to accommodate[21]. The National Flood Insurance Program (NFIP) compensates insured losses subject to policy terms and limits[22]. These instruments serve different purposes, but their maps, design thresholds and coverage do not directly describe how often individual streets, homes or stations actually flood.

Existing research reveals important gaps between mapped hazard, exposure and financial protection. Studies of flood insurance and flood equity mainly examine national patterns and annual averages[23–25]. A city-scale assessment of coastal, riverine and rainfall flooding in Los Angeles demonstrates substantial and unequal exposure beyond the federal floodplain[26]. National models now map rainfall flood hazard[6], and FEMA's insurance pricing incorporates property-level catastrophe models[14]. These advances broaden the representation of risk, but modelled hazard and loss remain distinct from observed recurrence at particular places. Loss records also provide an incomplete account of flooding whose consequences are uninsured or not readily assigned a monetary value[27]. What remains unresolved is how flood sources, exposed assets, losses and management instruments compare within one city on a common frequency basis, and how those comparisons relate to observed flooding. Dense street-sensor observations, combined with hydraulic stormwater maps, now make this comparison possible in New York City.

Here we examine how well the flood map, the drainage design standard and public flood insurance, together with conventional estimates of building loss, represent where New York City floods repeatedly and which people and assets are exposed. We combine public street-sensor observations, radar rainfall, hydraulic stormwater maps, the federal flood map, a coastal surge model, building and infrastructure inventories and insurance records[15,28–35] (Methods). The surge model is evaluated against Hurricane Sandy without calibration to observed losses. Using flood frequency as a common basis for comparison, we assess where each source causes flooding, which assets it reaches and the spatial, design and financial limits of the three instruments. This approach distinguishes the geography of rare-event losses from the places that experience recurrent flooding. We then discuss how a place-based measure of flood frequency could inform existing risk management.

Results

We address four questions: where and how often flooding occurs, whether loss estimates identify exposed populations and assets, how management instruments align with recurrent flooding, and how insurance coverage changes as losses grow.

Distinct geographies and frequencies of urban flooding

Storm surge, tide and rainfall affect different, partly overlapping parts of New York City. Coastal still-water inundation (surge plus tide) follows the shoreline and connected low-lying land (Fig. 1a). The extreme scenario in the city's stormwater flood maps instead follows buried streams and topographic lows in central Queens, Brooklyn and the Bronx. Of this rainfall footprint, 72% lies outside even the modelled 1-in-1,000-year surge reach. The two footprints are therefore largely separate, rather than nested.

The sources' observed frequencies also differ, and both are unevenly distributed across sensors. Throughout, a flood is a sensor event whose water takes at least 30 min to drain, so brief ponding is not counted (Methods). Since November 2020, half of FloodNet's tidally influenced sensors have flooded on fewer than four days per year, while a few flood on more than twenty. Most rain-responsive sensors have recorded no flood of this duration, and most of the rest flood less than twice a year (Fig. 1b). These statistics describe monitored locations rather than a representative sample of the city (Methods). Most tidal sensors lie within the federal flood zone, showing that where tidal flooding recurs, it occupies the same shoreline as rarer coastal inundation.

Rainfall flooding is uncommon, mostly shallow and concentrated in a few storms: rain-responsive sensors recorded a flood on 311 of 40,379 rainy sensor-days, water reached 1 ft on 54 of them, and the five largest storm days account for 56% of the flooding since late 2024 (Extended Data Fig. 1b). Its occurrence also depends strongly on location (Extended Data Fig. 1c; Supplementary Note 1). Near the shore, high tide is associated with approximately threefold higher odds of flooding at a given rainfall intensity (95% interval 1.4–7.3; Extended Data Fig. 1e). Flood probability rises steadily with hourly rainfall, and flooding begins well below the drainage design intensity (Extended Data Fig. 1c).

Combining the hydraulic footprints with sensor-informed frequency estimates reveals differences that the footprints alone do not show (Methods; Supplementary Note 1). Estimated street flooding of any depth at a typical basement lot in the rainfall footprint occurs approximately once every six years, compared with once every 40 years for a typical lot within the modelled 1-in-100-year surge reach (Fig. 1b; Fig. 2c; Extended Data Fig. 1d). These estimates describe street inundation at the lots, rather than water entering the dwellings. Rainfall flooding thus differs from coastal inundation in both geography and recurrence.

Flood losses and exposure follow different geographies

Modelled economic loss is concentrated in waterfront buildings and rare coastal events. Structure loss from surge remains small at frequent water levels and rises steeply for rarer events, yielding an expected annual loss of USD 485 million (5th–95th percentile range, USD 304–799 million; Fig. 2; Extended Data Fig. 2c; Supplementary Table 1). Without calibration to Sandy observations or

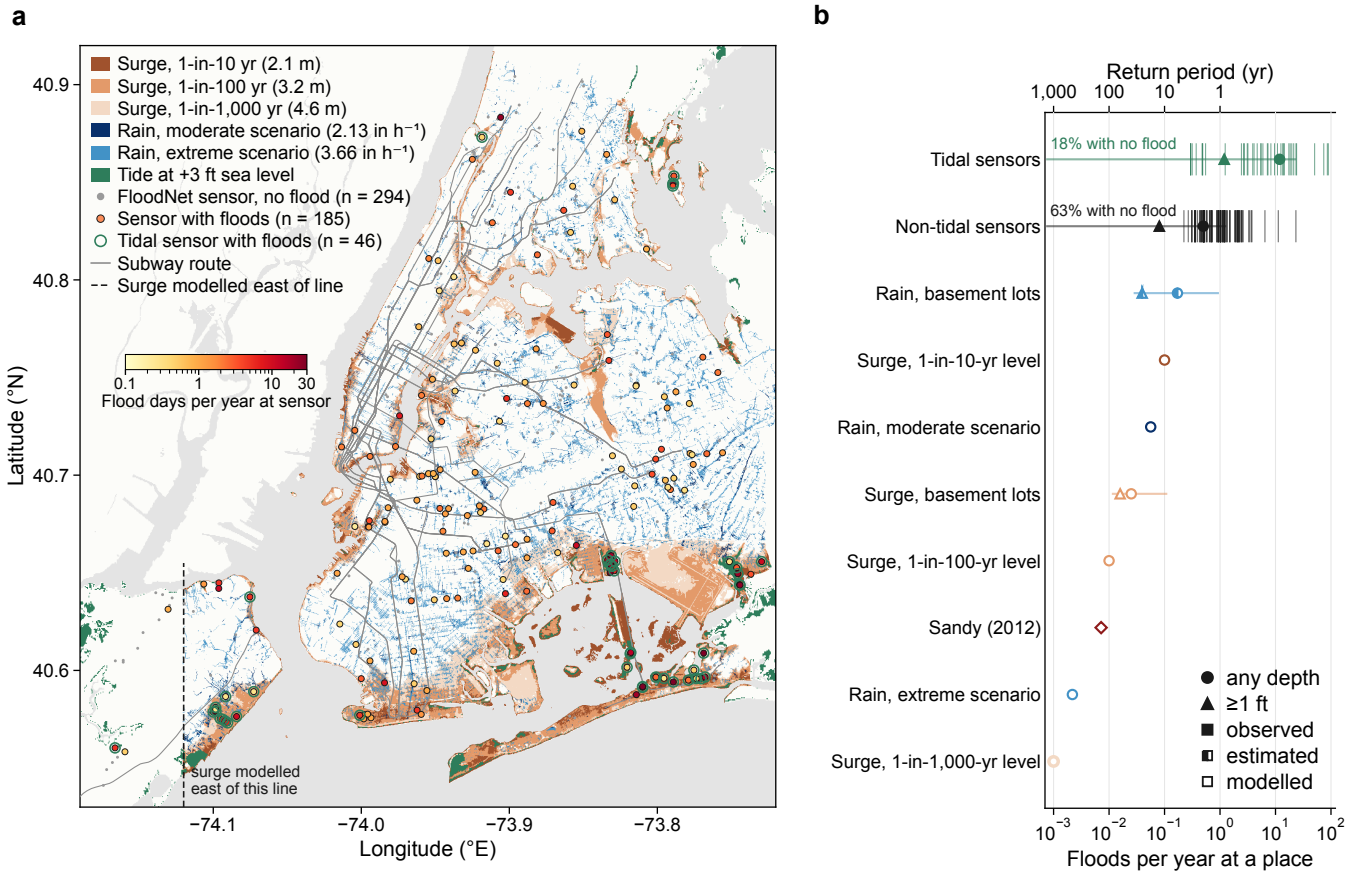


Fig. 1 Flood footprints and observed flood frequency by source. In both panels, observed and estimated frequencies count a flood as a sensor event whose water takes at least 30 min to drain. **a**, Flood footprints in the five boroughs: coastal still water (surge plus tide) at the 1-in-10, 1-in-100 and 1-in-1,000-yr levels (dark to light brown), the moderate and extreme rainfall scenarios (design intensities 2.13 and 3.66 in h^{-1}; dark and light blue) and land tidally inundated at +3 ft of sea-level rise (green). Dots, FloodNet sensors ($n = 479$), coloured by the observed flood days per year (grey, no flood recorded); green rings mark tidally influenced sensors that recorded a flood ($n = 46$); grey lines, subway routes. Present-day sea level, no coastal defences; surge is modelled east of the dashed line. **b**, Floods per year at a place (bottom axis) and return period (top axis), by source; circles, any depth; triangles, 1 ft or more; filled, observed; half-filled, estimated from observed rates; open, modelled; dark-red diamond, Hurricane Sandy. Sensor rows give network-wide rates (tidal, $n = 49$; non-tidal, $n = 304$), one tick for each sensor that recorded a flood and the share of sensors that recorded none; basement-lot rows give the typical lot in the extreme rainfall footprint ($n = 22{,}443$; storm-and-place model, long-run rainfall) or the median lot in the 1-in-100-yr surge reach ($n = 20{,}178$); lines, 10th to 90th percentile across sensors or lots, for rainfall lots across places. Rows are drawn in the colours of the corresponding layers in **a**; scenario rows give the frequency at the footprint edge, which for the rainfall scenarios is the return period of the design intensity on the National Oceanic and Atmospheric Administration (NOAA) Atlas 14 curve at Central Park (Methods).

losses, the model reproduces the hurricane's inundation footprint, and its damage chain gives a structure loss within the range implied by the city's damage estimate (Extended Data Fig. 2a,b).

Basement exposure differs from economic loss in both its frequency distribution and geography. More frequent coastal events account for a larger share of annual basement-lot exposure than of annual structure loss (Fig. 2b). The modelled 1-in-100-year surge reach and the extreme rainfall footprint each contain approximately 20,000 basement lots, yet fewer than one in ten of the rainfall-exposed lots also lies within that surge reach (Fig. 2a; Extended Data Fig. 3a;

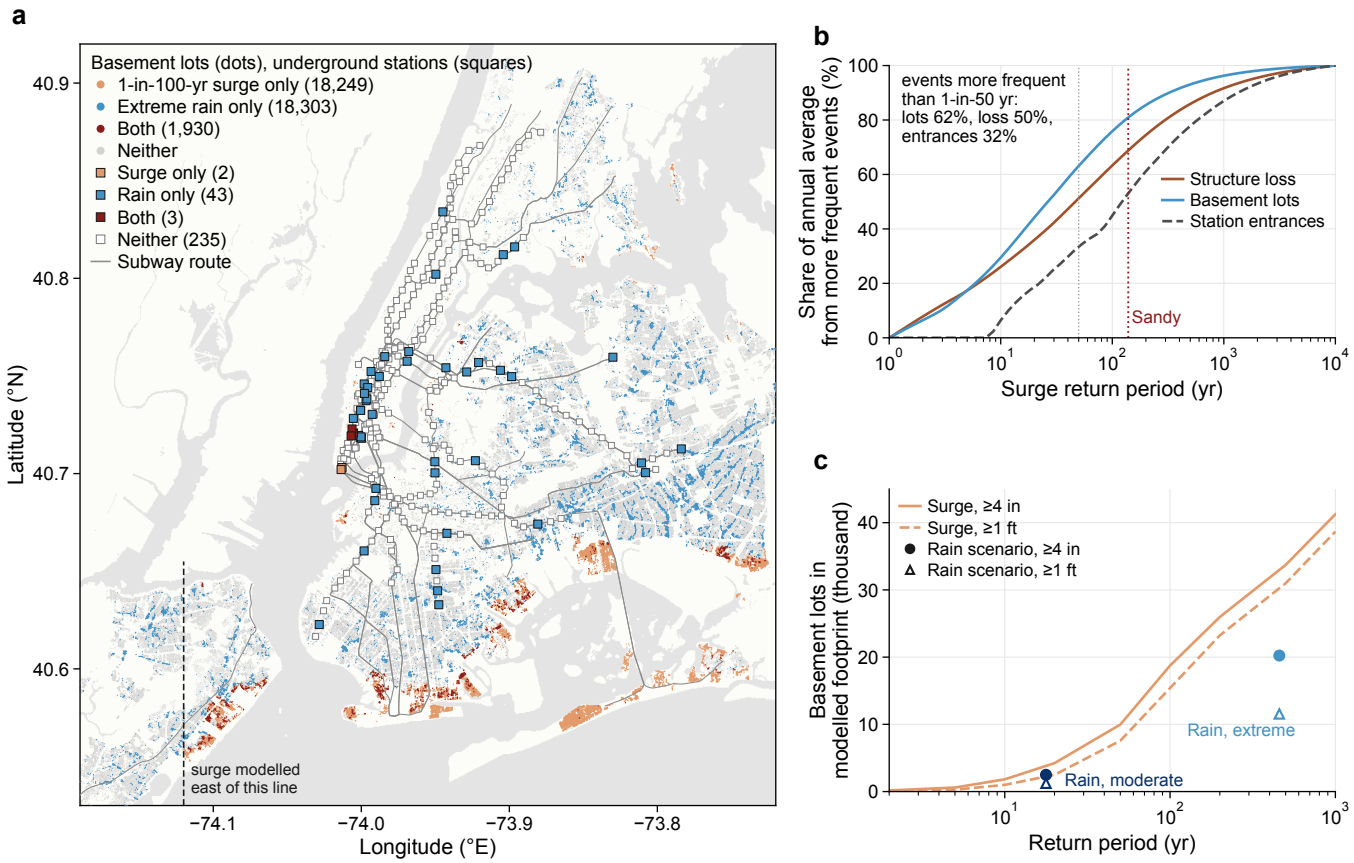


Fig. 2 Basement homes and the subway in the surge and rainfall footprints. a, Small-residential lots with a below-grade basement (dots) and underground subway stations (squares) inside the 1-in-100-yr surge reach only (orange), the extreme rainfall footprint only (blue), both (dark red) or neither (grey dots, open squares), counted where surge is modelled (east of the dashed line); grey lines, subway routes. **b**, Share of the annual average of structure loss (n = 881,621 structures), basement lots and street entrances of underground stations inside the surge footprint that comes from events more frequent than each surge return period; dotted lines, the 1-in-50-yr level and Hurricane Sandy. **c**, Basement lots flooded to 4 in or more (solid line, filled circles) or 1 ft or more (dashed line, open triangles) in the modelled surge footprint, by return period, and in the moderate and extreme rainfall scenarios, where surge is modelled. Rainfall return periods are those of each scenario's design intensity; the extreme scenario is run at 2080 sea level; the surge footprint has no defences.

Supplementary Table 1). Both groups are concentrated in Queens and Brooklyn, but occupy largely distinct shoreline and inland locations (Extended Data Fig. 3b).

Underground subway stations show a similar spatial contrast. The extreme rainfall footprint reaches 46 stations, compared with five within the modelled 1-in-100-year surge reach. These counts identify potentially exposed stations, rather than confirmed station flooding, and are based on each station's mapped location rather than on its entrances or other openings (Methods).

Economic loss and exposure consequently describe different dimensions of flood risk. Coastal structure-loss estimates highlight waterfront buildings and rare events, while rainfall flooding exposes a largely separate set of basement lots and subway stations inland. The recurrent street flooding identified in the sensor-informed analysis adds a frequency dimension that coastal structure loss alone does not capture.

Gaps in flood risk management coverage

Flood maps, drainage standards and public insurance serve different purposes, and each captures a different part of flood risk (Fig. 3a). The federal flood zone excludes most rainfall-exposed land and assets: 93% of the extreme rainfall footprint and 97% of its basement lots lie outside it, as do nearly all exposed subway stations. This spatial mismatch persists under the moderate rainfall scenario at current sea level and when alternative coastal flood boundaries are used (Supplementary Table 2).

Observed flooding also occurs predominantly below the drainage design intensity. At rain-responsive sensors, 93% of recorded flood days had hourly rainfall below that threshold (95% interval 88–98%), as did 70% of the days on which water reached 1 ft. When shorter rainfall peaks were considered, a substantial share of all flood days, though few of the 1-ft days, remained below it (Supplementary Fig. 1e–g). This proportion partly reflects the greater frequency of lighter rainfall; it does not by itself demonstrate failure under design conditions. Nevertheless, the design intensity alone does not describe the observed recurrence of flooding or its association with tidal water levels near the shore. Tidal flooding presents a different mismatch: most monitored tidal locations lie within the flood zone, and many of them flood repeatedly, which the mapped boundary alone does not distinguish.

NFIP participation is strongly associated with the flood-zone boundary (Fig. 3b). There are 62 policies per 100 buildings inside the zone, compared with two outside, and the contrast persists within Sandy's inundation footprint. In the extreme rainfall scenario, estimated payments from existing policies cover only 0.8% of modelled building loss in block groups predominantly outside the surge reach, compared with 10.6% in those predominantly inside it. This contrast persists across alternative policy allocations and spatial classifications (Supplementary Fig. 2b; Supplementary Table 2). These estimates concern building loss; they do not establish the financial protection available to basement occupants, for whom NFIP coverage is restricted[22].

The gaps therefore differ across instruments. Rainfall-exposed assets largely fall outside the federal flood zone, much observed flooding occurs below the drainage design intensity, and public insurance participation is sparse outside the mapped zone. Frequent tidal flooding, meanwhile, occurs largely within that zone, showing that inclusion within a mapped boundary does not by itself describe recurrent exposure.

Insurance gaps widen in larger flood events

For modelled surge losses, the share that existing NFIP coverage could pay declines as events grow (Fig. 4a,b). Even under an allocation that places all available coverage on damaged buildings, the estimated upper bound falls from 68% of loss for a 1-in-10-year event to 28% for a 1-in-1,000-year event (Supplementary Methods). Available coverage is fixed by the policies in force, while modelled loss rises steeply with water level (Extended Data Fig. 4a).

Estimated payments are lower when policy allocation is constrained. Randomly assigning policies among buildings within each block group yields payments covering 18% of expected annual structure loss (Supplementary Fig. 2). As a historical comparison, NFIP building claims after

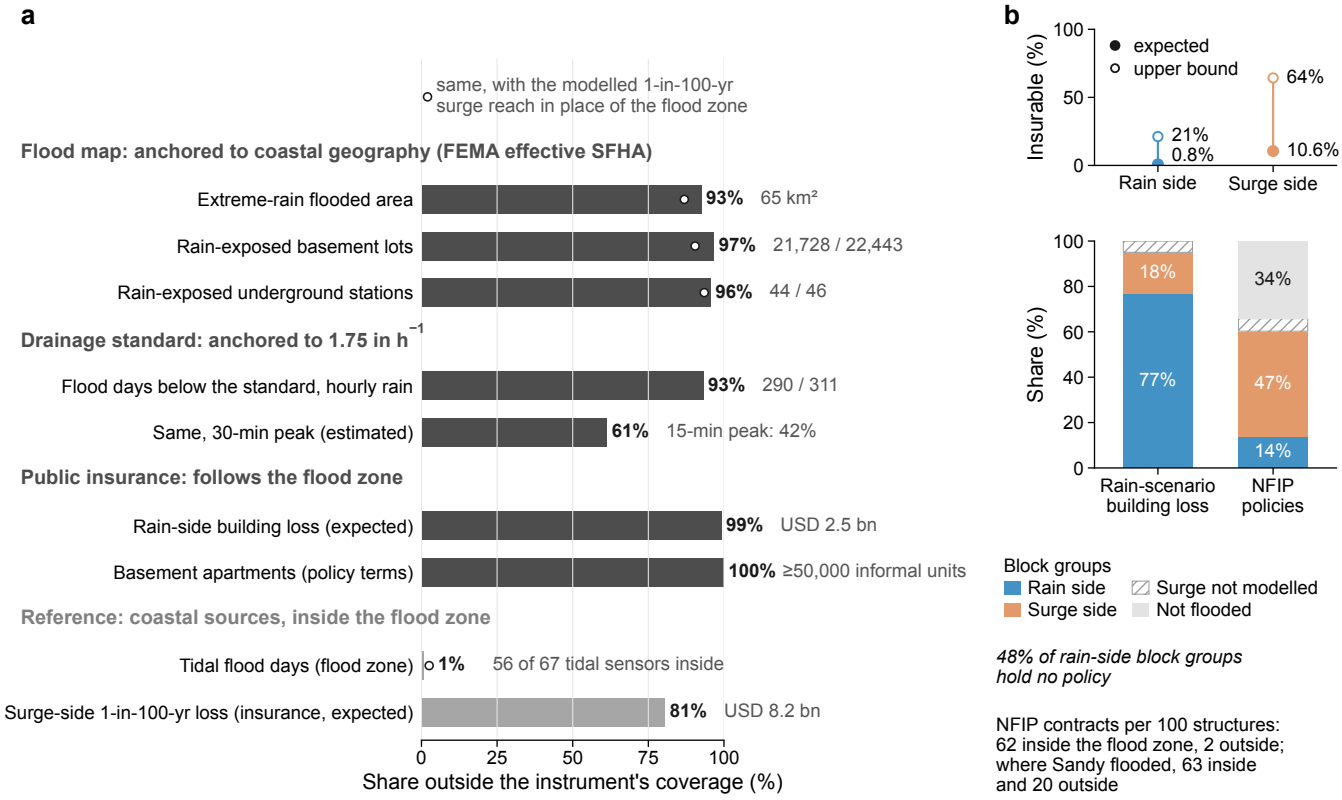


Fig. 3 Coverage of the exposure by each risk-management instrument. a, Share of exposure outside the coverage of each instrument, grouped by instrument: outside the flood zone in force (Special Flood Hazard Area, SFHA, of the Federal Emergency Management Agency, FEMA), below the 1.75 in h^{-1} drainage design intensity or outside public flood insurance; labels give numerator and denominator (area, loss or n). Grey bars are coastal sources inside the flood zone: tidal flood days at sensors outside the zone, and surge-side building loss at the 1-in-100-yr level outside expected insurance. **b**, Top, insurable share (the share of building loss that policies in place could pay) in the extreme rainfall scenario for rain-side and surge-side block groups, which have less than half or at least half of building value within the 1-in-1,000-yr surge reach; expected, policies placed at random within a block group; upper bound, every policy on a damaged building. Bottom, shares of building loss in that scenario and of National Flood Insurance Program (NFIP) policies (n = 36,961) by block-group type.

Sandy amounted to approximately one-tenth of modelled structure loss within the observed inundation footprint (Extended Data Fig. 4b).

Counterfactual scenarios distinguish limited participation from insufficient coverage (Fig. 4c). If every building carried its block group's mean policy coverage, estimated payments would rise from 18% to 48% of annual loss. Increasing coverage on every building to the applicable statutory maximum would raise that share to 58% and remove the decline in the covered share with event size across the modelled events (Fig. 4b). Wider participation therefore produces the larger improvement, but coverage amounts and statutory limits also constrain financial protection. Even with universal participation and maximum coverage, a substantial share of modelled structure loss would remain unpaid.

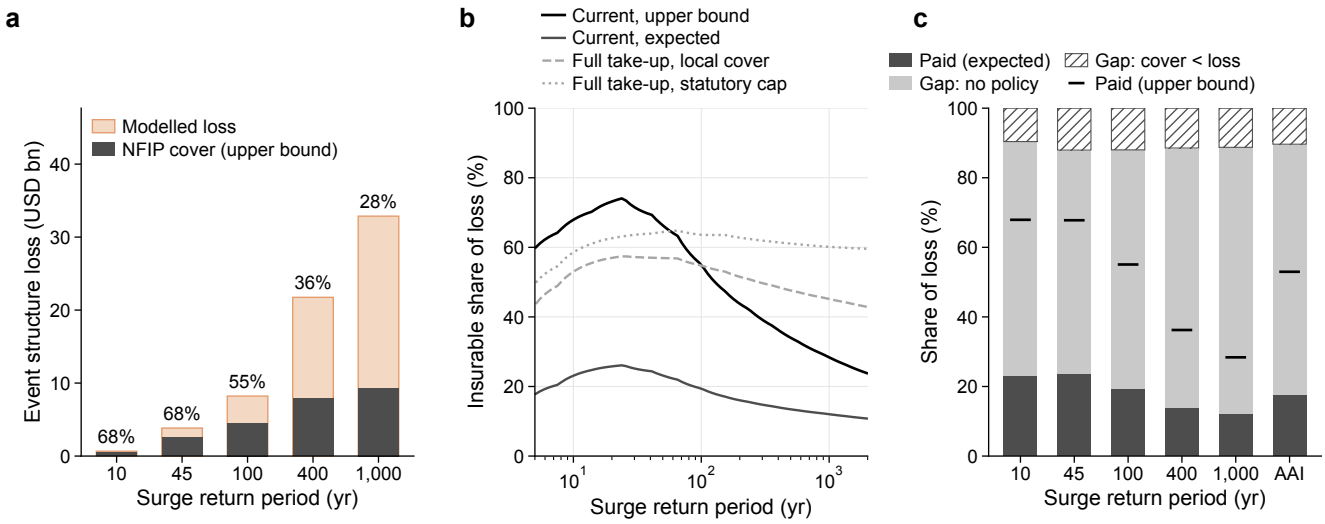


Fig. 4 Modelled surge loss and National Flood Insurance Program cover. Building cover of the National Flood Insurance Program (NFIP) is compared with modelled surge loss by block group (n = 36,961 policies in force). The upper bound places every policy on a damaged building; the expected value places policies at random within a block group. **a**, Event structure loss and the upper bound on insurance payment at five surge return periods; labels give that bound as a share of loss. **b**, Insurable share of loss against return period for current policies and for full participation at the block group's mean cover or at the statutory limit of USD 250,000 per residential unit. **c**, Event loss and annual average impact (AAI) divided into expected payment, a gap from buildings with no policy and a gap where cover is smaller than loss. Private insurance is not included.

Discussion

What the instruments do not index

Viewed through coastal building losses, New York City's flood risk is dominated by storm surge: a public-data model reproduces Sandy without calibration to observed losses. Street-level observations reveal a complementary picture of recurrent tidal and rainfall flooding. Rainfall flooding extends inland to homes and stations beyond the surge footprint, with 93% of the extreme-rainfall footprint outside the federal flood zone. Tidal flooding occurs within that zone but repeatedly affects shoreline places. These differences reflect the distinct purposes of flood maps, drainage standards and insurance. Their mapped boundaries, design thresholds and coverage do not directly describe the observed frequency of flooding at individual places.

A frequency layer for each instrument

The remedy is not to replace the coastal metric but to add the layer it lacks: how often each place floods, read from observation rather than inferred from a design event. For the flood map, the city's stormwater maps already resolve the rainfall footprint, and observed frequency (Fig. 1b) could show which parts of it flood often enough to carry requirements. The same applies to shoreline places inside the flood zone that already flood on ordinary tides. For the drainage standard, the target would become how often a place floods rather than whether a design storm is exceeded, as the city's cloudburst programme begins to do. Chronic ponding calls primarily for drainage, maintenance and adaptation measures; insurance alone is poorly suited to managing

predictable, recurrent losses. For insurance, the rare rainfall event is insurable, yet purchase is required only inside the flood zone, although FEMA now prices policies by property rather than by zone[14]. Where insurance already applies, wider participation matters more than a higher cap (Fig. 4b,c).

The layer has three immediate uses. The observed flood days per year at each sensor (Fig. 1a) can be published as an advisory as they stand. Overlaid on the basement lots and stations of Fig. 2, they give a priority list. And they can key requirements to observed recurrence rather than to a design storm. The layer needs an observation system sited to measure frequency rather than to confirm known trouble spots; today's sensors are 8.1 times denser inside the rainfall footprint than citywide (Extended Data Fig. 1a). Away from sensors the layer is a distribution rather than a value for each lot, which is why the network must be sited for it.

Generality and limitations

The analysis can be repeated where comparable hazard maps, exposure inventories, insurance records and flood observations are available. The underlying question extends beyond New York: how well do mapped hazards, design thresholds and insurance coverage represent the flooding repeatedly experienced at particular places? The extent and consequences of any mismatch remain empirical questions for each city.

Several limitations bound the numbers, and two bear on the conclusions. First, FloodNet sensors are preferentially located where flooding is expected and measure street water rather than basement inundation. Their observations therefore do not provide a representative estimate of flooding frequency across the city. Conversely, treating days without observations as dry may underestimate frequency at monitored sites. The record spans only six years, and estimates of longer-term rainfall flood frequency depend on rescaling against longer rainfall records (Methods). Second, the surge footprint is a static flood of land connected to the sea, without waves or defences. It overstates reach behind barriers and understates it where waves matter, so we report only block-group aggregates. The other limitations affect magnitudes. Loss excludes contents, business interruption and transit disruption, so the uninsured burden is understated. Informal basement units are allocated, not observed, from a citywide total uncertain by a factor of two. Private flood cover is not in the NFIP file, so the insurable shares bound public cover only. Tidal flooding is not traced to basement dwellings, for which no tidal footprint exists. Impacts on basements, the subway and ponding below the design intensity are not monetised, because no defensible damage function exists; building loss is the only impact compared in dollars.

What the city controls

The floods that recur in New York City are the ones its instruments do not index, and tidal flooding among them is becoming more frequent. Sea-level rise turns occasional tidal flooding into routine flooding[8,9], and 3 ft of rise would put 16 km^2 of land now dry at high tide under an ordinary one (Fig. 1a). Rainfall flooding also threatens renters in informal basement units, whose exposure and consequences are not fully represented by building-loss and insurance-coverage metrics[5]. These are also the floods over which the city holds the most direct levers. Surge loss turns on federal maps and coastal defences. Rainfall and tidal flooding turn on the city's own

stormwater maps, its drainage standard, where it places its sensors and how many of its residents are insured.

Conclusion

Comparing flood sources, exposed assets and management instruments on a common frequency basis reveals gaps that coastal loss estimates alone do not describe. Rainfall flooding extends beyond the federal flood zone, while tidal flooding repeatedly affects places within it. A place-based measure of observed flood frequency would complement existing assessments and help identify priorities for drainage, adaptation and financial protection. Street sensors and stormwater maps provide a starting point, but extending this information across the city requires representative monitoring and explicit treatment of uncertainty. The resulting frequency layer would connect flood risk management more closely to the flooding residents experience.

Methods

Study framework and data. The study area is the five boroughs of New York City. We place three flood sources (coastal surge, rainfall and tide), the assets they reach (buildings, basement dwellings and subway stations) and three risk-management instruments (the flood map, the drainage standard and public flood insurance) on one frequency axis. Every input is a public product, no hazard or damage parameter is calibrated to New York loss, and Hurricane Sandy (October 2012) is used only to validate the surge model. The impact calculation follows the hazard, exposure and vulnerability structure of the CLIMADA platform[36] and is implemented in Python; elevations are referenced to the North American Vertical Datum of 1988 (NAVD88). The hazard inputs are the still-water return-period curves of the USACE North Atlantic Coast Comprehensive Study (NACCS)[15,16], NOAA's CUDEM elevation model[37], the NOAA tide gauge at The Battery[38], NOAA's sea-level-rise inundation product[39], the Stormwater Flood Maps of the New York City Department of Environmental Protection (DEP)[31], NOAA Atlas 14 rainfall frequencies[40] and NOAA Multi-Radar Multi-Sensor radar rainfall[32]. Street flooding is observed by FloodNet, 479 ultrasonic sensors logging events since 2020[3]; 311 street-flooding complaints[41,42] serve only to test the observation system. Exposure and vulnerability come from the USACE National Structure Inventory (NSI)[28] and USACE generic depth–damage functions[29,30], PLUTO, the city's tax-lot database[43], an estimate of unauthorised dwelling units[4,44], the tract share of low-to-moderate-income (LMI) households from the US Department of Housing and Urban Development[45,46], and subway stations and entrances from the Metropolitan Transportation Authority (MTA)[47–49]. The instruments are represented by FEMA's National Flood Hazard Layer, with the 2015 Preliminary Flood Insurance Rate Map as a check[35,50], and by the National Flood Insurance Program (NFIP) policy and claim files[33,34]; validation uses the field-verified Sandy inundation extent[51,52] and the city's Sandy damage estimate[53,54]. Identifiers, versions, access dates, filters and record counts are in the Supplementary Methods and Supplementary Table 3. Depths and rainfall are given in US customary units, in which the city's standards and maps are defined (1 in = 25.4 mm; 1 ft = 0.305 m).

Flood hazards and recurrence. *Coastal surge.* Surge frequency is a return-period curve of still-water level, not of storm category: the mean NACCS curve at The Battery, digitised and converted to NAVD88 (Extended Data Fig. 2d), on which Sandy's observed peak of 3.44 m NAVD88 is a 1-in-140-year level. Curves at three other save points change the annual loss by about 2%, so the single curve is retained (Extended Data Fig. 2e,f; Supplementary Methods). For each of 29 water levels from 0.5 to 7.5 m, the flooded area is the set of 20 m elevation cells below the water level and hydrologically connected to the open sea, and depth is water level minus ground elevation; this static (bathtub) flood[55] has no bulkheads, seawalls or post-Sandy defences and overstates inundation at low water levels. To place surge on the frequency axis, each cell is assigned the return period of the lowest water level that floods it to any depth, to 4 in or to 1 ft.

Rainfall. The DEP maps give hydraulic-model footprints for a moderate scenario (design rainfall of 2.13 in h^{-1}, current sea level) and an extreme one (3.66 in h^{-1}, 2080 sea level), each divided into nuisance (4 in to 1 ft) and deep ($\geq$1 ft) flooding. The city describes them as roughly 10- and 100-year storms[56]; we index both, and the 1.75 in h^{-1} sewer design intensity[21], on one source, the NOAA Atlas 14 60-minute intensity–frequency curve at Central Park, by interpolating between its tabulated return periods: about 18 years for the moderate scenario, 458 years for the extreme (between the 200- and 500-year intensities, 3.21 and 3.70 in h^{-1}) and 7 years for the design intensity. These are return periods of a rainfall intensity at one gauge; the extreme scenario adds 2080 sea level, so they locate the scenarios on the axis rather than give the flood frequency at any place. The design intensity is exceeded about yearly over 30 min, so hourly rain is the averaging time that matches the standard and sub-hourly peaks are a sensitivity (Supplementary Note 2).

Observed tidal and rainfall flooding. A flood is a FloodNet event (a run of one-minute depth readings above 10 mm) whose water takes at least 30 min to drain from its maximum depth. No public standard sets a duration. We use 30 min so that brief, shallow wetting is not counted as a flood: it lies within the range of drain times (15 to 60 min) above which floods draw more 311 complaints, and rainfall predicts flood days almost as well with it as with every event. The choice changes how often flooding is counted, most strongly at shallow depths, and its effect is reported as a sensitivity (Supplementary Fig. 1a–d; Supplementary Methods). Events at sensors missing from the sensor table, and events at non-tidal sensors with no rain at the sensor or at the city's gauges, are removed and listed with reasons in the released data[57]. FloodNet flags 64 sensors as tidally influenced; three more within 1 km of open water whose floods on dry days mostly begin at a high tide are treated as tidal (Supplementary Methods). Of 2,929 recorded events, 2,104 are counted. Tide is read from these sensors rather than modelled: each is located relative to the flood zone and to the modelled surge reach, and the highest water level at The Battery since 2020 is compared with the NACCS curve; tidal inundation under sea-level rise (+3 ft above mean higher high water) is not coupled to the surge runs, which use present-day sea level.

Frequency definitions and comparability. The axis carries three different quantities. For surge, the frequency at a place is the annual exceedance probability of the lowest water level that floods it, counting one flood day per exceedance. At a sensor, the observed flood-day rate is the number

of distinct days with a flood divided by the years the sensor was online, for sensors online for at least six months (49 tidal, 304 non-tidal); days rather than events are counted so that tidal and rain sensors share a unit, and rates are summarised by the median and the 10th to 90th percentile across sensors because events are concentrated. At a basement lot, the estimated long-term flood-day frequency comes from the model below, with rainfall rescaled to long-run rates. All three are expressed as expected flood days per year at any depth, 4 in or 1 ft (Fig. 1b), but they rest on different data and assumptions; they are compared to rank sources and to separate frequent from rare flooding, not as statistically equivalent estimates.

Exposure and loss assessment. *Building losses.* Each building takes its NSI replacement value and the depth of its 20 m cell less its first-floor height, and its damage is read from one of four USACE functions (one storey or more, with or without a basement); for buildings above three storeys the functions apply to the share of value in the lowest three storeys (3/N; alternatives in Extended Data Fig. 2g–i). Only structure value is counted: contents, business interruption, transit disruption and damage inside basement dwellings are excluded, so building loss understates the burden on the households and infrastructure counted below. Surge loss is computed at the 29 water levels and integrated over exceedance probability from 1 to 10^{-4} to give the annual average impact (AAI); rainfall building loss uses the same buildings and functions, with depth set by footprint class.

Residential exposure. Basement lots are one-to-three-family houses and small walk-ups with a full or partial below-grade basement in PLUTO, counted inside a footprint by the cell under the lot centroid (citywide for rainfall, where surge is modelled for surge). Informal basement units have no register: we allocate a lower bound of 50,000 units (the city's figure for basement apartments) and an upper bound of 114,000 (the citywide estimate of unauthorised units, which is not limited to basements) to basement lots uniformly, in proportion to the tract's LMI share or in proportion to that share above 30%, and report the range across rules (Extended Data Fig. 3a; Supplementary Table 1).

Infrastructure exposure. An underground station is counted as exposed when its MTA station coordinate lies in a footprint. Water would enter through street entrances and ventilation gratings, and only the entrances have public locations: counting a station when any of its street entrances lies in a footprint gives 95 stations in the extreme rainfall footprint and six in the 1-in-100-year surge reach, against 46 and five. Station counts therefore indicate potential exposure rather than flooding, and all figures are exposure without defences.

Comparability. To compare the hazard models like for like, basement lots are counted inside the surge footprint at each return period and inside the two rainfall scenarios at the same depth thresholds (4 in and 1 ft), where surge is modelled (Fig. 2c). The timing of each impact along the surge axis is the share of its annual average that comes from events more frequent than a given return period (Fig. 2b).

Modelling recurrent rainfall flooding. To estimate how often rain floods a basement lot without a sensor, we model the rainy sensor-days at non-tidal sensors (radar total of at least 0.1 in). For sensor s on day d, logit $P(\text{flood}) = \beta_{b(s,d)} + \gamma_1 H_d + \gamma_2 H_d N_s + v_s$, where b is one of four bins

of the day's maximum hourly radar intensity at the sensor (Extended Data Fig. 1c), H_d indicates a high tide (The Battery above mean higher high water within 2 h of the peak rain hour), N_s indicates a sensor within 1 km of open water, and $v_s \sim \mathcal{N}(0, \sigma_v^2)$ is a sensor-specific intercept drawn from a common distribution across places (a random effect); the model is fitted separately at each depth threshold. Adding a random effect for the storm day shows that places differ at least as much as storms (Supplementary Note 1). The tide effect is tested separately, for sensors within 1 km of open water and inland, by the logistic regression logit $P(\text{flood}) = \alpha_s + \beta_{b(s,d)} + \gamma H_d + \delta I_d$, where α_s is a separate intercept for each sensor (a fixed effect) and I_d is the storm's citywide peak intensity; standard errors are clustered by storm day. The rain model uses a distribution of sensor intercepts because its aim is prediction at lots without sensors, for which an intercept can be drawn from that distribution. The tide test uses a separate intercept for each sensor because its aim is a comparison of days with and without a high tide at the same sensor, which removes all differences between places. The two approaches give consistent tide effects: both find that a high tide raises the odds of flooding about threefold near open water and has no detectable effect inland (Supplementary Note 1). The expected number of flood days per year at a lot is $\sum_b n_b \left[(1 - \pi_b)\, p_b + \pi_b\, p_b^H\right]$, where n_b is the rainy days per year in bin b at the lot's radar cell, π_b the share of rainy sensor-days in bin b with a high tide, and p_b, p_b^H the flood probabilities without and with a high tide at a typical place ($v_s = 0$) with the lot's value of N; drawing v_s for each lot gives the spread across places. Because heavy hourly rain was unusually frequent in 2020–2026, n_b in the two upper bins is rescaled to NOAA Atlas 14 rates and in the two lower bins to the 2013–2019 gauge record. Intervals come from refitting the model on resampled storm days, since a storm floods many sensors at once. Sensors are sited where flooding is expected, so these frequencies likely overstate flooding at a typical place; they are used to rank sources, not to map them, and their transfer between boroughs and dependence on the averaging time of rainfall are tested in Supplementary Notes 1 and 2.

Model validation and uncertainty. The surge chain is checked against Sandy in two parts. The modelled footprint at Sandy's peak level is scored against the field-verified inundation zone within the five boroughs, where that zone exists, and contains the same five underground stations (Extended Data Fig. 2a). The exposure and damage chain applied to the observed zone, with depth set to the peak level minus ground elevation, gives an uncalibrated structure loss of USD 10.5 bn, compared with the city's estimate of USD 19 bn for damage and lost activity[53,54]: taking direct physical loss as 60–70% of the total and contents as 9–30% of that gives an observed structure-only loss of 8.0–12.1 bn (Extended Data Fig. 2b). This validates the surge chain at one water level only; the rainfall and tidal frequencies come from observation and are not tested by Sandy. Uncertainty in the surge AAI is propagated with 4,000 draws over the curve digitisation, structure valuation, the damage-function family and its scaling to the observed Sandy range (distributions in Supplementary Table 4; Extended Data Fig. 2c). The resulting interval does not include the structural assumptions of no coastal defences, a single water-level curve and present-day sea level, which are stated rather than sampled, and no second validation event exists for New York (Supplementary Methods). The observation system is tested separately: sensor siting by the share of sensors inside the extreme rainfall footprint relative to the footprint's share of city land (Extended Data Fig. 1a), the duration criterion against complaints and rainfall (Supplementary

Fig. 1a–d), and the transfer of flood rates between boroughs by holding out each borough in turn (Supplementary Fig. 1h).

Flood risk management and insurance coverage. *Flood map.* Coverage is the share of the extreme rainfall footprint area, of the basement lots inside it and of the underground stations inside it that lie outside the Special Flood Hazard Area (SFHA; zones A, AE, AH, AO, V and VE of the map in force), with the share outside the modelled 1-in-100-year surge reach as a check (Fig. 3a); the 2015 Preliminary Flood Insurance Rate Map, which the city's building code applies where it is more restrictive, is treated in the same way (Supplementary Table 2).

Drainage standard. Coverage is the share of observed flood days at non-tidal sensors whose maximum hourly intensity is below the 1.75 in h^{-1} design intensity, with a sensor-clustered bootstrap interval (Supplementary Note 2).

Insurance. Policy coordinates are redacted, so joins are made at the census block group. Take-up inside the flood zone is the number of NFIP contracts (policies) rated in an A or V zone per NSI structure inside the SFHA, and outside it the remaining contracts per structure outside, also computed for block groups with at least half of their structures in the observed Sandy zone; because contracts include condominium units and rated zones can predate the current map, these are contracts per structure, not the share of buildings insured. Sandy claims are NFIP claims for losses of 28 October to 5 November 2012 in the five boroughs (Extended Data Fig. 4b). Insurable shares are computed for each block group and water level. The upper bound on payment is min(block-group structure loss, block-group building cover), which puts every insured dollar on a damaged building. The expected value is a scenario estimate of payment under random placement: each structure carries a policy with probability equal to the block group's contracts per structure (capped at 1) and, if insured, recovers min(its structure loss, the block group's mean cover per contract); this assumes that holding a policy is independent of loss within a block group and ignores deductibles and contents. The shortfall then splits, structure by structure, into a no-policy term, (1 − take-up) × loss, and a cover term, take-up × max(loss − mean cover, 0). Two counterfactuals are evaluated in the same way: full take-up at the block group's mean cover per contract, and full take-up at the statutory limit (USD 250,000 per residential unit, USD 500,000 for non-residential buildings). All quantities are integrated to annual values (Fig. 4; Supplementary Table 5), and two alternative placements, by rated zone and by largest loss first, test the independence assumption (Supplementary Note 3). For the rainfall overlay (Fig. 3b; Supplementary Table 6), a block group is surge-side if at least half of its structure value lies inside the 1-in-1,000-year still-water reach and rain-side otherwise; block groups with less than half of their structure value where surge is modelled are not classed, and those with no building loss in the extreme scenario form a fourth group (other thresholds, the 1-in-100-year reach and the moderate scenario are in Supplementary Table 2). For income, block groups are aggregated to census tracts and grouped by LMI share (Supplementary Fig. 3).

Data availability

All inputs are public; their providers, identifiers and access dates are listed in Supplementary Table 3 and in the repository README. The cleaned FloodNet street-flood record, with every

excluded event and the reason for its exclusion, is archived at Zenodo[57] under CC BY 4.0. The intermediate products of this study and the results behind every figure and table are available at https://github.com/cbian-prog/nyc-recurrent-flood-protection and archived at Zenodo[58] under CC BY 4.0. The public inputs as retrieved for this study are archived at Zenodo[59], except the NACCS per-save-point files, which the US Army Corps of Engineers distributes after registration. This work uses the FEMA OpenFEMA API but is not endorsed by FEMA.

Code availability

The Python code that reproduces every analysis, figure and table, with the order in which to run it, is available at https://github.com/cbian-prog/nyc-recurrent-flood-protection and archived at Zenodo[58] under the MIT licence.

Acknowledgements

We thank the FloodNet project (New York University and the City University of New York) for making its street-level flood sensor data publicly available, and the US Army Corps of Engineers Coastal Hazards System for access to the NACCS save-point products.

Funding

This work received no specific funding.

Author contributions

C.B. conceived and designed the study, developed the methods, wrote the code, collected and curated the data, performed the analyses and validation, produced the figures, wrote the manuscript and managed the project. D.N.B. and T.Z. reviewed and edited the manuscript. All authors approved the final version.

Competing interests

The authors declare no competing interests.

References

[1] Yuan, A., Spira-Cohen, A., Olson, C. & Lane, K. Immediate injury deaths related to the remnants from Hurricane Ida in New York City, September 1–2, 2021. *Disaster Med. Public Health Prep.* **18**, e55 (2024).

[2] Frank, T. Deaths from Hurricane Ida expose flaws in FEMA flood maps. *E&E News / Scientific American* (October 2021).

[3] Mydlarz, C. et al. FloodNet: low-cost ultrasonic sensors for real-time measurement of hyperlocal, street-level floods in New York City. *Water Resour. Res.* **60**, e2023WR036806 (2024).

[4] City of New York, Extreme Weather Response Task Force. *The New Normal: Combating Storm-Related Extreme Weather in New York City* (City of New York, 2021).

[5] Kramer Mills, C., Nair, A. & di Giovanni, J. Flood-prone basement housing in New York City and the impact on low- and moderate-income renters. *Liberty Street Economics* (Federal Reserve Bank of New York, 17 November 2023).

[6] Wing, O. E. J. et al. Estimates of present and future flood risk in the conterminous United States. *Environ. Res. Lett.* **13**, 034023 (2018).

[7] Rosenzweig, B. R. et al. Pluvial flood risk and opportunities for resilience. *WIREs Water* **5**, e1302 (2018).

[8] Sweet, W. V. & Park, J. From the extreme to the mean: acceleration and tipping points of coastal inundation from sea level rise. *Earth's Future* **2**, 579–600 (2014).

[9] Thompson, P. R. et al. Rapid increases and extreme months in projections of United States high-tide flooding. *Nat. Clim. Change* **11**, 584–590 (2021).

[10] Moftakhari, H. R., AghaKouchak, A., Sanders, B. F. & Matthew, R. A. Cumulative hazard: the case of nuisance flooding. *Earth's Future* **5**, 214–223 (2017).

[11] Merz, B., Kreibich, H., Schwarze, R. & Thieken, A. Assessment of economic flood damage. *Nat. Hazards Earth Syst. Sci.* **10**, 1697–1724 (2010).

[12] Aerts, J. C. J. H., Botzen, W. J. W., Emanuel, K., Lin, N., de Moel, H. & Michel-Kerjan, E. O. Evaluating flood resilience strategies for coastal megacities. *Science* **344**, 473–475 (2014).

[13] Federal Emergency Management Agency. *Hazus Flood Model Technical Manual, Hazus 6.1* (FEMA, July 2024).

[14] Federal Emergency Management Agency. *National Flood Insurance Program Risk Rating 2.0: Methodology and Data Sources* (FEMA, 2021).

[15] Nadal-Caraballo, N. C., Melby, J. A., Gonzalez, V. M. & Cox, A. T. *North Atlantic Coast Comprehensive Study (NACCS): Coastal Storm Hazards from Virginia to Maine.* ERDC/CHL TR-15-5 (US Army Engineer Research and Development Center, 2015).

[16] Cialone, M. A. et al. *North Atlantic Coast Comprehensive Study (NACCS) Coastal Storm Model Simulations: Waves and Water Levels.* ERDC/CHL TR-15-14 (US Army Engineer Research and Development Center, 2015).

[17] Orton, P. M. et al. A validated tropical–extratropical flood hazard assessment for New York Harbor. *J. Geophys. Res. Oceans* **121**, 8904–8929 (2016).

[18] Garner, A. J. et al. Impact of climate change on New York City's coastal flood hazard: increasing flood heights from the preindustrial to 2300 CE. *Proc. Natl Acad. Sci. USA* **114**, 11861–11866 (2017).

[19] Aerts, J. C. J. H., Lin, N., Botzen, W., Emanuel, K. & de Moel, H. Low-probability flood risk modeling for New York City. *Risk Anal.* **33**, 772–788 (2013).

[20] Dixon, L., Clancy, N., Bender, B., Kofner, A., Manheim, D. & Zakaras, L. *Flood Insurance in New York City Following Hurricane Sandy*. RR-328 (RAND, 2013).

[21] New York City Department of Environmental Protection. *Stormwater Resiliency in a Changing Climate*. Testimony before the New York City Council Committee on Environmental Protection, Resiliency and Waterfronts (NYC DEP, 22 October 2025).

[22] Federal Emergency Management Agency. *National Flood Insurance Program Dwelling Form: Standard Flood Insurance Policy*. FEMA F-122 (effective 1 October 2021; 44 CFR Part 61, Appendix A(1)).

[23] Amornsiripanitch, N., Biswas, S., Orellana-Li, J. & Zink, D. Measuring flood underinsurance in the USA. *Nat. Clim. Change* **15**, 971–977 (2025).

[24] Bradt, J. T., Kousky, C. & Wing, O. E. J. Voluntary purchases and adverse selection in the market for flood insurance. *J. Environ. Econ. Manag.* **110**, 102515 (2021).

[25] Wing, O. E. J. et al. Inequitable patterns of US flood risk in the Anthropocene. *Nat. Clim. Change* **12**, 156–162 (2022).

[26] Sanders, B. F. et al. Large and inequitable flood risks in Los Angeles, California. *Nat. Sustain.* **6**, 47–57 (2023).

[27] Gall, M., Borden, K. A. & Cutter, S. L. When do losses count? Six fallacies of natural hazards loss data. *Bull. Am. Meteorol. Soc.* **90**, 799–810 (2009).

[28] US Army Corps of Engineers. *National Structure Inventory (NSI) 2026 Base: Technical Documentation* (USACE Hydrologic Engineering Center, nsi.sec.usace.army.mil, 2026).

[29] US Army Corps of Engineers. *Economic Guidance Memorandum (EGM) 01-03, Generic Depth-Damage Relationships* (CECW-PG, 4 December 2000).

[30] US Army Corps of Engineers. *Economic Guidance Memorandum (EGM) 04-01, Generic Depth-Damage Relationships for Residential Structures with Basements* (CECW-PG, 10 October 2003).

[31] New York City Department of Environmental Protection. NYC Stormwater Flood Maps. NYC Open Data https://data.cityofnewyork.us/d/9i7c-xyvv (2024).

[32] Zhang, J. et al. Multi-Radar Multi-Sensor (MRMS) quantitative precipitation estimation: initial operating capabilities. *Bull. Am. Meteorol. Soc.* **97**, 621–638 (2016).

[33] Federal Emergency Management Agency. OpenFEMA Dataset: NFIP Redacted Policies – v3. OpenFEMA https://www.fema.gov/openfema-data-page/nfip-redacted-policies-v3 (2026).

[34] Federal Emergency Management Agency. OpenFEMA Dataset: NFIP Redacted Claims – v3. OpenFEMA https://www.fema.gov/openfema-data-page/nfip-redacted-claims-v3 (2026).

[35] Federal Emergency Management Agency. National Flood Hazard Layer (NFHL). FEMA https://hazards.fema.gov/arcgis/rest/services/public/NFHL/MapServer (2026).

[36] Aznar-Siguan, G. & Bresch, D. N. CLIMADA v1: a global weather and climate risk assessment platform. *Geosci. Model Dev.* **12**, 3085–3097 (2019).

[37] Cooperative Institute for Research in Environmental Sciences. *Continuously Updated Digital Elevation Model (CUDEM) – 1/9 Arc-Second Resolution Bathymetric-Topographic Tiles* (NOAA National Centers for Environmental Information, 2014); https://doi.org/10.25921/ds9v-ky35.

[38] Center for Operational Oceanographic Products and Services. Station 8518750, The Battery, NY: Datums and Verified Water Levels. NOAA Tides and Currents https://tidesandcurrents.noaa.gov/stationhome.html?id=8518750 (2026).

[39] Office for Coastal Management. NOAA Office for Coastal Management Sea Level Rise Data: 1–10 ft Sea Level Rise Inundation Extent. NOAA National Centers for Environmental Information https://www.fisheries.noaa.gov/inport/item/48106 (2026).

[40] Perica, S. et al. *NOAA Atlas 14, Volume 10, Version 3.0: Precipitation-Frequency Atlas of the United States, Northeastern States* (NOAA National Weather Service, 2015; revised 2019).

[41] Agonafir, C., Pabon, A. R., Lakhankar, T., Khanbilvardi, R. & Devineni, N. Understanding New York City street flooding through 311 complaints. *J. Hydrol.* **605**, 127300 (2022).

[42] Smith, B. & Rodriguez, S. Spatial analysis of high-resolution radar rainfall and citizen-reported flash flood data in ultra-urban New York City. *Water* **9**, 736 (2017).

[43] New York City Department of City Planning. Primary Land Use Tax Lot Output (PLUTO). NYC Open Data https://data.cityofnewyork.us/d/64uk-42ks (2026).

[44] Sheth, R. & Neuwirth, R. *New York's Housing Underground: A Refuge and Resource* (Pratt Center for Community Development and Chhaya Community Development Corporation, 2008).

[45] US Department of Housing and Urban Development. ACS 5-Year 2016–2020 Low- and Moderate-Income Summary Data. HUD Exchange https://www.hudexchange.info/programs/acs-low-mod-summary-data/ (2024).

[46] New York City Department of City Planning. Community Development Block Grant (CDBG) Eligibility by Census Tract. NYC Open Data https://data.cityofnewyork.us/d/qmcw-ur37 (2026).

[47] Metropolitan Transportation Authority. MTA Subway Stations. Open NY https://data.ny.gov/d/39hk-dx4f (2024).

[48] Metropolitan Transportation Authority. MTA Subway Entrances and Exits: 2024. Open NY https://data.ny.gov/d/i9wp-a4ja (2024).

[49] Metropolitan Transportation Authority. New York City Transit Subway Static GTFS Feed. MTA Developer Resources https://www.mta.info/developers (2026).

[50] Federal Emergency Management Agency. Preliminary Flood Insurance Rate Map, New York City, DFIRM 360497, issued 30 January 2015. FEMA Flood Map Service Center https://hazards.fema.gov/femaportal/prelimdownload/ (2015).

[51] FEMA Modeling Task Force. *Hurricane Sandy Storm Surge Extent, Final Field-Verified High Resolution* (FEMA, 2013).

[52] NYC Department of Small Business Services. Sandy Inundation Zone. NYC Open Data https://data.cityofnewyork.us/d/5xsi-dfpx (2015).

[53] City of New York. *PlaNYC: A Stronger, More Resilient New York* (Special Initiative for Rebuilding and Resiliency, 2013).

[54] Office of the New York City Comptroller. *Ten Years After Sandy: Barriers to Resilience* (Bureau of Policy and Research, 2022).

[55] Vousdoukas, M. I. et al. Developments in large-scale coastal flood hazard mapping. *Nat. Hazards Earth Syst. Sci.* **16**, 1841–1853 (2016).

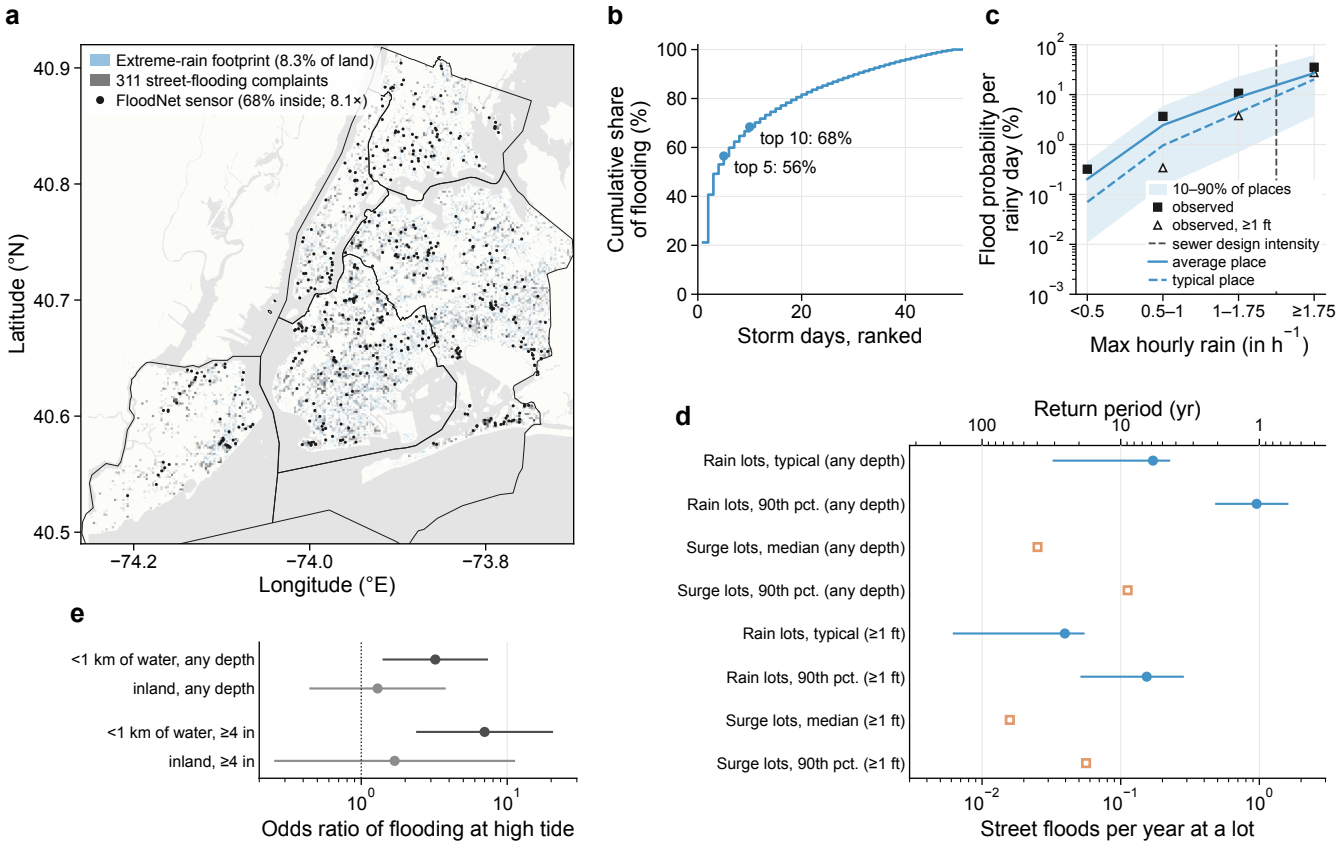
[56] NYC Mayor's Office of Resiliency. *New York City Stormwater Resiliency Plan: Helping New Yorkers Understand and Manage Vulnerabilities from Extreme Rain* (City of New York, 2021).

[57] Bian, C. Cleaned FloodNet street-flood record, New York City, 2020–2026. Zenodo https://doi.org/10.5281/zenodo.23964158 (2026).

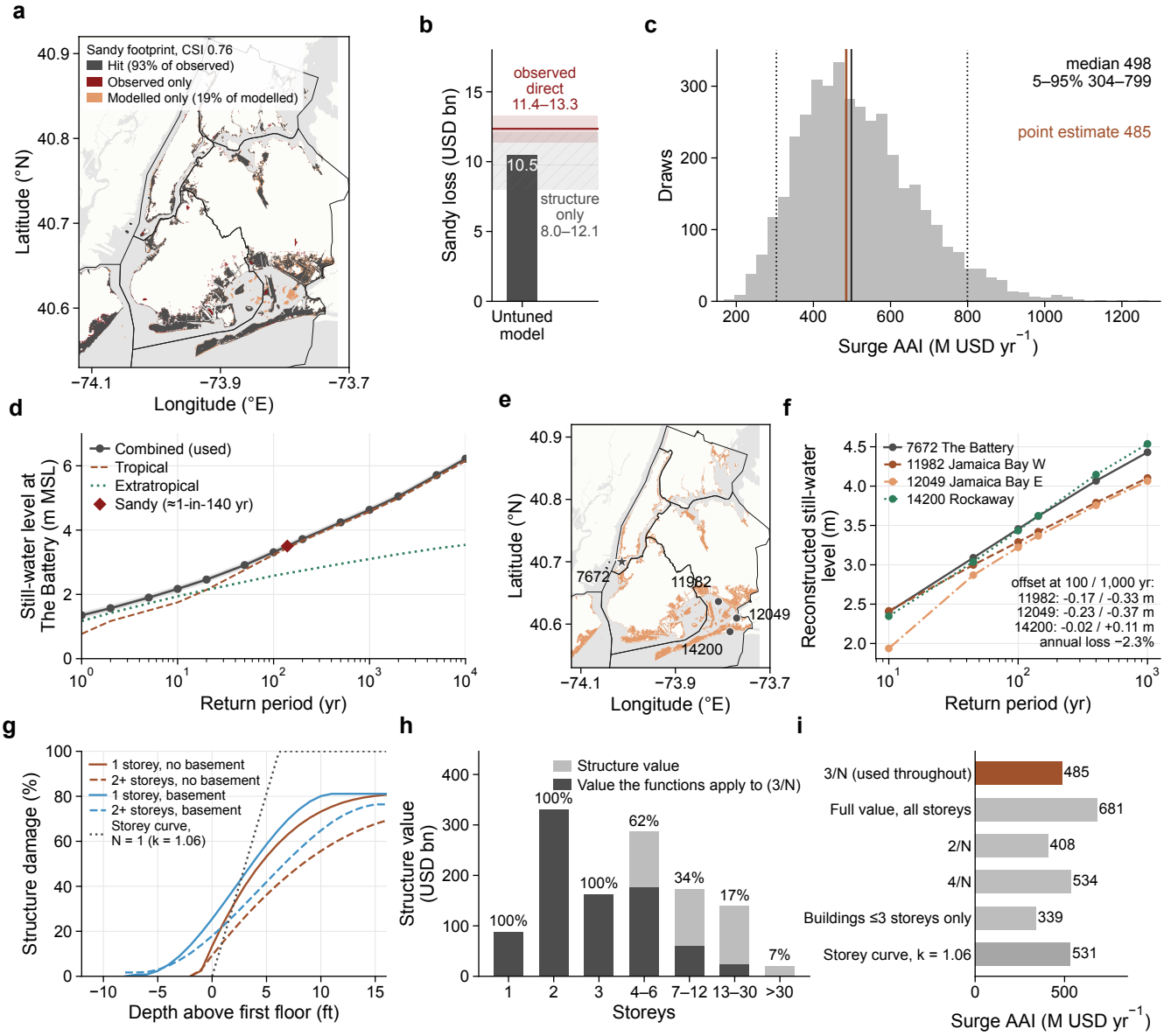
[58] Bian, C. Code and data for: Recurrent flooding beyond the reach of flood risk management in New York City. Zenodo https://doi.org/10.5281/zenodo.23962188 (2026).

[59] Bian, C. Public inputs as retrieved for: Recurrent flooding beyond the reach of flood risk management in New York City. Zenodo https://doi.org/10.5281/zenodo.23962247 (2026).

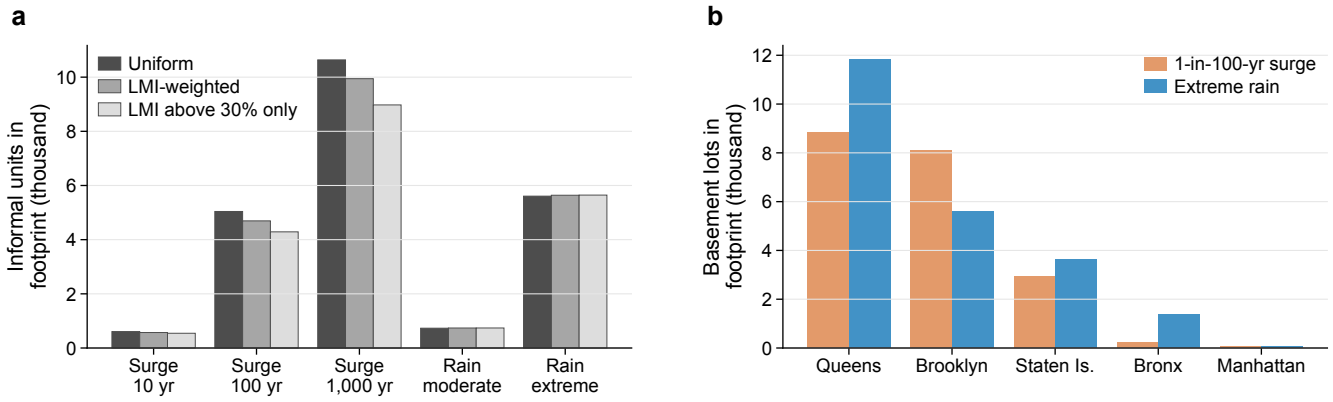
Extended Data



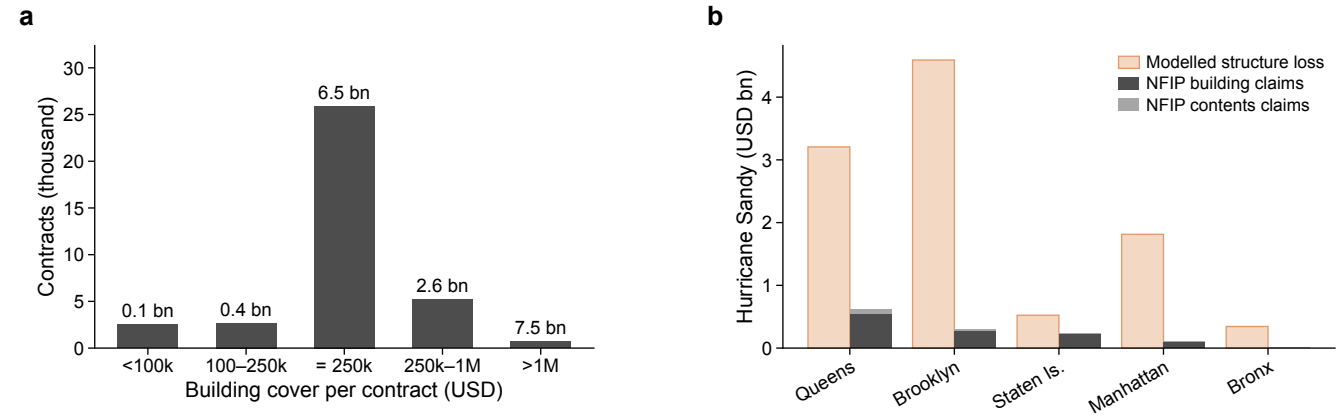
Extended Data Fig. 1 Reading the street-flood record: sensor siting, storms and places. Street floods are events whose water takes at least 30 min to drain, as in Fig. 1. **a**, Street-flooding complaints to the city's 311 service line on a 200 m grid (log scale; $n = 21{,}287$, 2020–2026) and FloodNet sensors ($n = 479$) over the extreme rainfall footprint; the legend gives the footprint's share of city land, the share of sensors inside it and their ratio. **b**, Cumulative share of flooding (share of reporting sensors flooded, summed over storm days) against storm days ranked, on the 137 rainy days with at least 100 sensors reporting (November 2024 to August 2026). **c**, Flood probability on a rainy day by maximum hourly radar rain at the sensor ($n = 40{,}379$ sensor-days with rain), observed over all sensor-days (no 1-ft flood in the lightest bin) and modelled as the average over places and for a typical place; band, 10th to 90th percentile of places; the 1.75 in h^{-1} design intensity is applied to hourly rain. **d**, Street floods per year at basement lots in the extreme rainfall footprint (long-run rainfall; lines, storm-day bootstrap 95% intervals) and modelled surge floods at lots inside the 1-in-100-yr reach. **e**, Odds ratio of flooding at a high tide (The Battery above mean higher high water within 2 h of the day's peak rain hour) at the same rain, with sensor fixed effects and the storm's citywide peak intensity held fixed; lines, storm-day clustered 95% intervals.



Extended Data Fig. 2 The surge model: validation, hazard curve and vulnerability. **a**, Modelled footprint at Sandy's observed peak (3.44 m above the North American Vertical Datum of 1988, NAVD88) compared with the field-verified 2012 inundation zone; CSI, critical success index. **b**, Sandy structure loss from the uncalibrated model, the observed direct-loss range including contents (line, centre) and the structure-only range implied by contents shares of 9–30%. **c**, Monte Carlo distribution of the annual average impact (AAI) of surge loss (n = 4,000 draws); vertical lines, median, 5th and 95th percentiles and point estimate. **d**, Still-water level above mean sea level (MSL) against return period at The Battery from the North Atlantic Coast Comprehensive Study (NACCS save point 7672, with the ±0.1 m digitisation band) and its tropical and extratropical components. **e**, The four NACCS save points over the 1-in-100-yr surge footprint. **f**, Still-water level by return period reconstructed at each point. **g**, Structure damage against depth relative to the first floor for the four US Army Corps of Engineers (USACE) generic depth-damage functions and for the storey-fraction curve (scale parameter k). **h**, Structure value by storey class and the value to which the functions are applied under the lowest-three-storeys rule (3/N); labels give the applied share. **i**, Surge AAI under alternative rules for applying the functions to taller buildings.



Extended Data Fig. 3 Basement homes: allocation and geography. a, Informal basement units inside each footprint when the citywide estimate of unauthorised units (an upper bound) is allocated to the small-residential basement lots uniformly, in proportion to the tract's low-to-moderate-income (LMI) share or in proportion to that share above 30%. **b**, Basement lots by borough inside the 1-in-100-yr surge reach (where surge is modelled) and the extreme rainfall footprint (citywide).



Extended Data Fig. 4 Why insurance falls short: policies and Sandy claims. a, National Flood Insurance Program (NFIP) contracts by building cover per contract (n = 36,961); labels give total cover per class. **b**, Hurricane Sandy: modelled structure loss on the observed footprint against NFIP building and contents claims paid, by borough (n = 16,498 claims, NFIP Redacted Claims v3).

Supplementary Files

This is a list of supplementary files associated with this preprint. Click to download.

- Supplementary.pdf